

INFLUENCE OF CARBONISATION TEMPERATURE ON THE SURFACE PORE CHARACTERISTICS OF ACID-TREATED OIL PALM EMPTY FRUIT BUNCH ACTIVATED CARBON

Article history

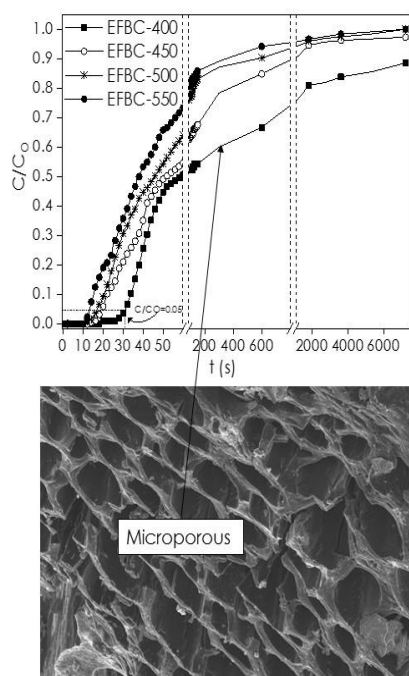
Received
27 February 2020
Received in revised form
3 August 2020
Accepted
9 August 2020
Published online
27 August 2020

Norhidayah Ahmad, Naimah Ibrahim*, Phan Yun Fu, Razi Ahmad

*Corresponding author
naimah@unimap.edu.my

School of Environmental Engineering, Universiti Malaysia Perlis, Kompleks Pusat Pengajian Jejawi 3, 02600 Arau, Perlis, Malaysia

Graphical abstract



Abstract

Carbonisation process affects the surface physical and chemical properties of an activated carbon. Therefore, this work aims to investigate the influence of carbonisation temperature from 400 to 550°C during activation with 85% phosphoric acid (H_3PO_4) on the surface pore characteristics of activated carbon produced from oil palm empty fruit bunch (EFB) for nitric oxide (NO) removal from gas streams. Pore and morphological characterisation showed that EFB carbonised at 400°C (EFBC-400) is microporous and has a uniform pore structure with 98% micropore volume. Increasing carbonisation temperature resulted in pore enlargement from 2.8 to 4.7 nm and increment in pore heterogeneity and BET surface area from 215 to 759 m^2/g . However, the NO breakthrough experiment indicated that EFBC-400 is more favourable for low-temperature NO removal, due to the importance of microporosity in adsorption of NO. Further study will look at the kinetics of NO removal and the adsorbent regeneration.

Keywords: Air pollution control, Oil palm empty fruit bunch, Carbonisation, Adsorption, Nitric oxide, Pore characterisation

Abstrak

Proses pengkarbonan mempengaruhi sifat fizikal dan kimia permukaan bagi suatu karbon teraktif. Justeru, kerja ini bertujuan untuk mengkaji pengaruh suhu pengkarbonan dari 400 hingga 550°C semasa pengaktifan dengan 85% asid fosforik (H_3PO_4) terhadap ciri-ciri liang permukaan karbon teraktif yang terhasil daripada tandan kosong (EFB) kelapa sawit untuk penyingkiran nitrik oksida (NO) daripada aliran gas. Pencirian liang dan morfologi menunjukkan EFB yang dikarbonkan pada 400°C (EFBC-400) adalah bermikroliang dan mempunyai struktur liang seragam dengan 98% isipadu mikroliang. Peningkatan suhu pengkarbonan menghasilkan pembesaran liang dari 2.8 ke 4.7 nm serta peningkatan dalam keheterogenan liang dan luas permukaan BET dari 215 ke 759 m^2/g . Namun, ujian bulus NO menunjukkan EFBC-400 adalah lebih baik untuk penjerapan NO bersuhu rendah disebabkan kepentingan mikroliang dalam penjerapan NO. Kajian seterusnya akan melihat kepada kinetik penyingkiran NO dan penjanaan semula penjerap.

Kata kunci: Kawalan pencemaran udara, Tandan kosong kelapa sawit, Pengkarbonan, Penjerapan, Nitrik oksida, Pencirian liang

© 2020 Penerbit UTM Press. All rights reserved

1.0 INTRODUCTION

Nitrogen oxides (NO_x), known cumulatively for nitric oxide (NO) and nitrogen dioxide (NO_2) are toxic gases as they are perilous to humans and the environment. The formation of acid rain, for example, is due to the reaction between water molecules in the atmosphere and nitrogen oxides (NO_x) or sulphur oxides (SO_x), which are largely emitted from industries and vehicles [1,2]. One of the methods developed for the treatment of NO_x is activated carbon adsorption. Activated carbon with well-developed pore structures is versatile and has been widely used as adsorbents, catalysts, and/or catalyst supports in many applications such as for pharmaceutical usage, gaseous storage or purification and separation, pollutants and odour removal, etc. [3–5]. The diversity of pore characteristics makes activated carbon suitable for different applications, e.g. activated carbon with microporous characteristics is more favourable for gaseous adsorption, while mesoporous one is more suitable for liquid pollutants due to the larger size of liquid molecules [6].

Activated carbon can be produced through physical or chemical activation [7], but method selection largely influences the pore characteristics, including the pore shapes, pore size distribution, and surface chemistry [8]. Physical activation is usually a two-step process; initially started with carbonisation of a carbonaceous precursor in inert condition, followed by activation at high temperature in the presence of activating agents e.g. carbon dioxide (CO_2) or steam [9]. Chemical activation is commonly a one-step process in which raw material gets carbonised and impregnated with a chemical agent at moderate temperature in air or inert atmosphere at the same time. Chemical activation requires lower energy and operating cost while producing higher carbon yields, high surface areas, and a well-developed porous structure. On the other hand, the surface chemistry on the carbon precursor can be modified with various activating agents such as NaOH [10,11], KOH [12], H_3PO_4 [13–15], and HNO_3 [16,17] to enhance surface oxygen complexes [18] which normally aid in the adsorption process.

The abundance of agricultural by-products makes them a good alternative for activated carbon precursors [19]. The use of carbonaceous materials for NO removal has been extensively studied including olive stone [20], date pits [21], walnut shell [22], rice straw and sewage sludge derived char [23], orange skin [24] palm shell [25] cherry stones [26] and coconut shell [18]. As the second-largest producer of crude palm oil in the world, Malaysia produces abundant oil palm biomass, e.g., frond and empty fruit bunch (EFB), which are commonly disposed in a landfill or used as organic fertilizer by leaving them mulching on plantation ground [26,27]. Oil palm EFB has high carbon content and is rich in lignin, thus, could be used as a precursor material for activated carbon production. Carbonisation temperature is among

critical activation process parameters as it could influence the complex carbon structure generated. This work aims to investigate the influence of carbonisation temperature on the surface pore properties of the activated carbon produced from EFB for low temperature NO removal.

2.0 METHODOLOGY

2.1 Activation and Carbonisation Process

Oil Palm EFB fibre collected from United Oil Palm Mill Sdn. Bhd, Nibong Tebal, Penang, Malaysia, was physically cleaned and dried at 110°C for about 24 hours to remove surface moisture before undergoing the chemical activation process. Initially, the raw EFB was soaked with concentrated phosphoric acid at 1:1 (wt./vol.) in a 1500 mL beaker for 30 minutes at room temperature, followed by carbonisation at different temperatures, i.e., 400, 450, 500 and 550°C in a furnace for 24 hours. The activated carbon produced from carbonisation of EFB (EFBC) was abbreviated as EFBC-400, EFBC-450, EFBC-500, and EFBC-550 based on their carbonisation temperatures, respectively. Afterward, the EFBC samples were cooled to room temperature and washed with copious hot distilled water to remove residual acid and left to dry in the oven overnight at 110°C . The dried EFBC was sieved to obtain average particle sizes between 0.5-1 mm for further testing.

2.2 Characterisation of EFBC

Nitrogen adsorption/desorption analysis was conducted at -196°C using a surface area and porosity analyser (Belsorp Mini II, Japan) based on BET method. Approximately 0.2 g of sample was used for the analysis and degassed at 300°C for 3 hrs under nitrogen flow. Following that, the Brunauer-Emmett-Teller (BET), t-plot and Barrett-Joyner-Halenda (BJH) methods were used to calculate the specific surface area, micropore volume and mesopore volume respectively, while the total pore volume was calculated from the N_2 adsorption-desorption isotherm. The volume of nitrogen held at the highest relative pressure ($p/p_0 = 0.99$) was used to determine the pore volume. The mesopore size distribution was determined based on the BJH method, while the micropore size distribution was obtained based on the micropore analysis method (MP-method).

In addition, the surface morphology of raw EFB and EFBC at different carbonisation temperatures was analysed using micrographs obtained at $5000\times$ magnification with Field Emission Scanning Electron Microscopy (FEI Nova NanoSEM 450).

2.3 NO Breakthrough Experiments

For breakthrough experiments, 5 g of EFBC sample was placed in the middle of a quartz column reactor with 1.5 cm internal diameter and 25 cm length, while the

rest of the empty space was filled with quartz wool. The schematic diagram of the experimental rig for NO breakthrough experiment was already shown in a previous work [28]. Nitric oxide (NO) breakthrough experiment was performed at 100°C using a 100 mL/min flow of 500 ppm NO, balanced with helium. All gases were supplied by Linde, Malaysia. The total flow rate was controlled using a mass flow controller (Aalborg Instruments, USA). The sample was initially flushed with helium for 1 hour, followed by a breakthrough test until equilibrium or for 2 hours. The inlet and outlet concentration of NO was measured using a NO gas analyser (TESTO 340, Germany). The gas analyser was pre-calibrated with zero (helium) and span (3000 ppm NO) gas before experiment. The NO adsorption capacity was calculated at the non-STP condition from the following dynamic mass balance equation (1).

$$q = \frac{Q_f t_f y_f}{m_c} \quad (1)$$

Where q is the adsorption capacity (mg/g), Q_f is the volumetric feed flow rate at STP (L/min), y_f is mole fraction of NO in the feed, m_c is the mass of EFBC samples (g).

The time equivalent, t_f to the adsorption capacity was obtained from equation (2):

$$t_f = \int_0^{\infty} \left(1 - \frac{C}{C_0}\right) dt \quad (2)$$

where t is the time at equilibrium, C is the concentration of NO at time t , and C_0 is the initial concentration of NO.

3.0 RESULTS AND DISCUSSION

3.1 Surface Area and Pore Characteristics

Figure 1 shows the nitrogen adsorption/desorption isotherms, while Table 1 shows the BET specific surface area (S_{BET}), micropore volume (V_{mic}), total pore volume (V_t), percentage of micropores (%) or ratio of micropore volume to total pore volume (V_{mic}/V_t) and average pore diameter (D_{ave}) of each sample at different carbonisation temperatures. The isotherm of EFBC carbonised at 400°C (EFBC-400) in Figure 1 shows a flat plateau shape, concave to the relative pressure (p/p_0) axis, with a limiting value as p/p_0 approaches 1, indicative of Type 1 isotherm. This indicates that monolayer adsorption is happening and shows that EFBC has the characteristic of microporous solids (pore size < 2 nm). From 450°C onwards, the curve started to transform towards a Type IV isotherm with a characteristic hysteresis loop, indicating that multilayer adsorption can be expected, together with capillary condensation that takes place in the mesopores.

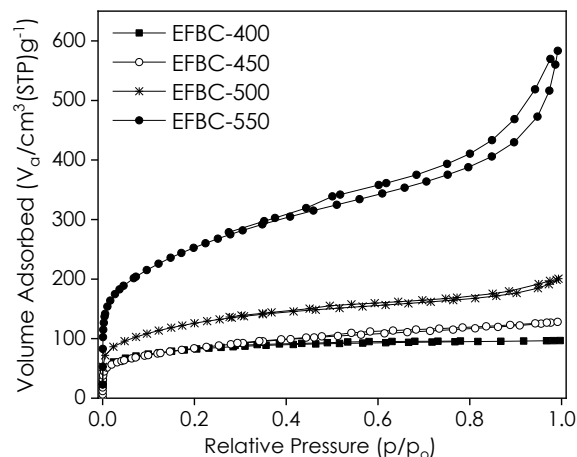


Figure 1 Nitrogen adsorption/desorption isotherm of EFBC at different carbonisation temperatures from 400 to 550°C

Table 1 Surface area and pore characteristics of EFBC carbonised at different temperatures between 400 to 550°C

Sample	S_{BET} (m^2/g)	V_{mic} (cm^3/g)	V_t (cm^3/g)	V_{mic} (%)	D_{ave} (nm)
EFBC-400	215	0.147	0.150	98.1	2.78
EFBC-450	246	0.174	0.198	88.1	3.22
EFBC-500	354	0.234	0.308	76.0	3.48
EFBC-550	759	0.482	0.890	54.1	4.69

As can be observed in Table 1, the average pore diameter increases from 2.8 to 4.7 nm, indicating that the pores are enlarged as the temperature of carbonisation rises. At the same time, the percentage of micropores also decreases from around 98 (at 400°C) to 54% (at 550°C). Table 1 also shows an increase in the S_{BET} from around 215 to 760 m^2/g , total micropore volume from 0.15 to 0.5 cm^3/g , and total pore volume from 0.15 to 0.9 cm^3/g as the carbonisation temperature increases from 400 to 500°C, implying that the carbon surface is becoming more porous. Several previous works also reported similar enhancement in the pore structure of the carbon matrix due to the increase in carbonisation temperatures [29,30]. Such changes in pore characteristics with temperature rise from 400 to 550°C could be due to the increase in the decomposition of volatile matters from the precursor material [31]. Besides, with the increase in carbonisation temperature, the surface complexes (e.g., oxygen and phosphate surface groups) responsible for further carbon gasification are also increased, leading to enlargement of pores from micro to mesopore size. During carbonisation, the residual acid on the precursor surface is also decomposed, leaving the carbon matrix in an expanded state with an accessible pore structure.

Figures 2 (a-b) show the pore size distribution of EFBC samples derived from BJH and MP-plot methods respectively. Figure 2(a) indicates that the pore size

distribution curve of EFBC-400 is high below the 2 nm radius, confirming its microporous characteristic. An increase in volume distribution (dV_p/dr_p) with r_p (up to 60 nm) can also be observed as the carbonisation temperature increases from 400 to 550°C, indicative of the increase in the pore heterogeneity. On the other hand, Figure 2(b) shows that increasing carbonisation temperature also influences the pore radius and heterogeneity in the lower size range, between 0.4-2 nm. Although the percentage of microposity is reduced due to enlargement of some of the pores, more micropores are actually produced at 550°C compared to the other samples.

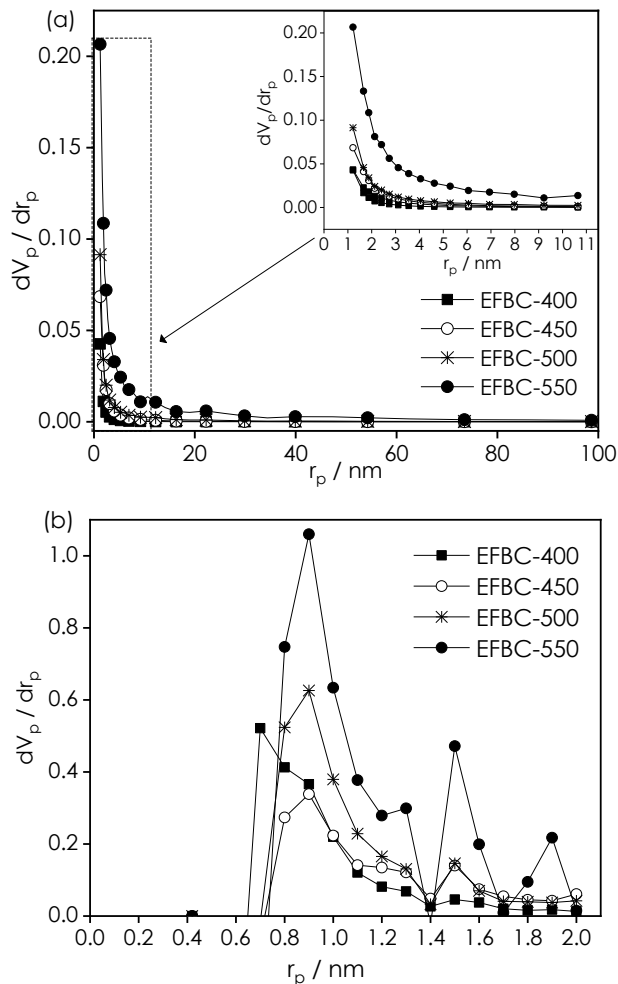


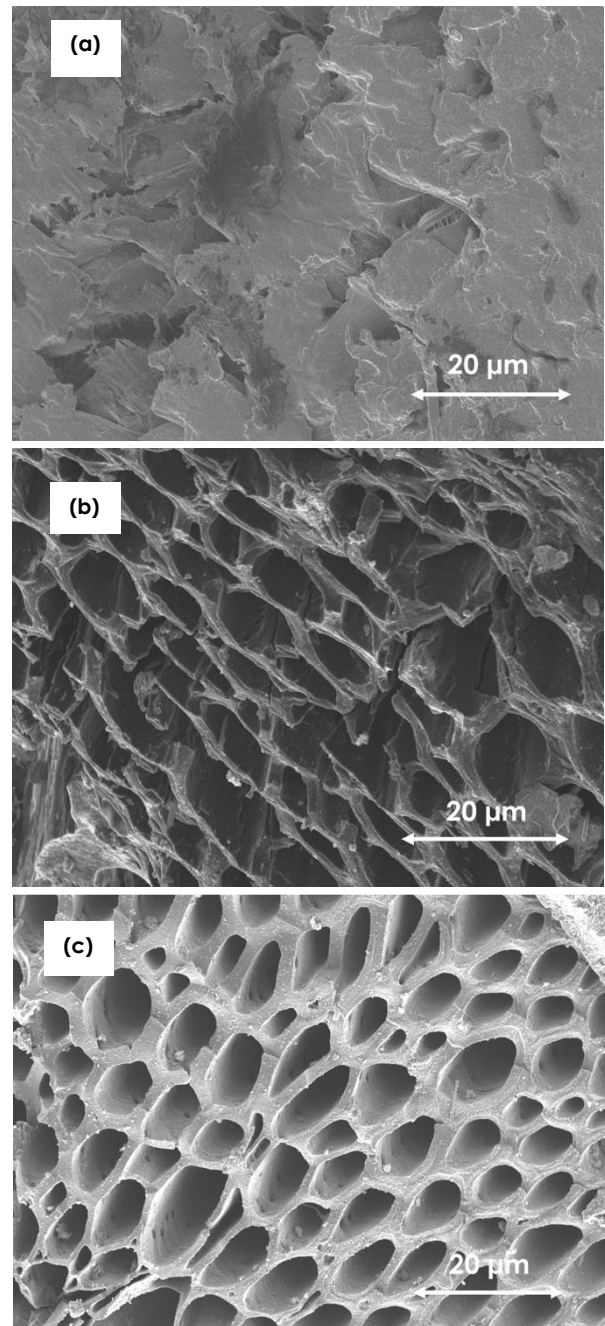
Figure 2 Mesopore (a) and micropore (b) size distributions of EFBC at various carbonisation temperatures obtained using BJH and MP methods

3.2 Surface Morphology

It has been shown in Section 3.1 that increasing carbonisation temperature results in the enlargement of pores and pore heterogeneity on the carbon complex, which are also reflected in the FESEM micrograph images shown in Figures 3(a-e) below. In Figure 3(a), the precursor material can be seen to

have a thick wall structure, which is non-porous, while all EFBC samples carbonised at 400 and 450°C showed in Figure 3(b-c) exhibit a well-developed porous structure with quite uniform pore diameter ranging from 5 to 10 μm at 5000 times magnification, corresponding to actual pore size around 1-2 nm.

The result indicates that activation of EFB with phosphoric acid (H_3PO_4) and heat treatment is successful in creating pores, which are expected to be favourable for adsorption of gaseous pollutants like NO_x . Like other chemical activating agents, H_3PO_4 plays an important role as a dehydrating agent that could penetrate deep into the carbon structure, resulting in the development of pores on the surface of activated carbon precursor [31].



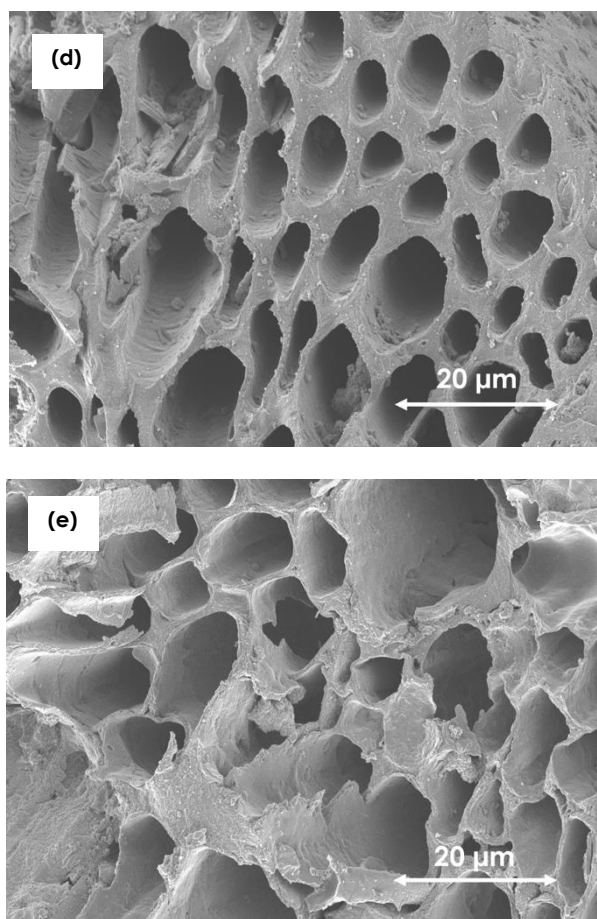


Figure 3 FESEM images of raw EFB and EFBC at different temperature of carbonisation at 5000x magnifications: (a) raw EFB, (b) EFBC-400, (c) EFBC-450, (d) EFBC-500, and (e) EFBC-550

At higher carbonisation temperatures (especially 500 and 550°C) shown in Figures 3(d-e), the pores are becoming less uniform, and some pores are becoming larger up to 20 µm (corresponding to 4 nm). As discussed earlier in Section 3.1, higher temperatures could play a more significant role in the decomposition of volatile matters and acid precursors.

3.3 NO Breakthrough Study

Finally, the resulting EFBC samples carbonised at varying temperatures were tested for NO removal under a mild condition with a 100 mL/min flow of 500 ppm NO at 100°C. In general, it can be observed from Figure 4 that the NO breakthrough curves become less gradual to achieve saturation with the increasing carbonisation temperatures. The time taken to achieve breakthrough point at $C/C_0=0.05$ also reduces from around 31 to 14 s as the carbonisation temperature increases from 400-550°C. On the other hand, Table 2 shows that the corresponding NO adsorption capacity by EFBC-400 after 2 hours of the experiment is 0.58 mg/g at maximum, and this

decreases to 0.14 mg/g with increasing temperature to 550°C (EFBC-550).

Apart from the well-understood influence of oxygen surface functional groups generated on EFBC due to pre-treatment with H_3PO_4 [3,6,32], which is not of debate here, these results indicate that the surface pore structure of EFBC also plays a role in NO removal at low temperature (100°C). In the previous sections, EFBC-400 has been shown to have the highest percentage of micropores, lower pore volume, lower average pore diameter and more uniform pore structures than the other samples.

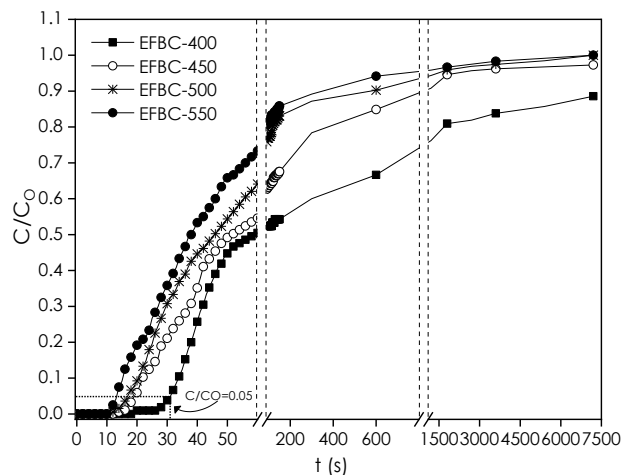


Figure 4 The breakthrough curves of EFBC at different carbonisation temperatures

Table 2 NO adsorption capacities of EFBC at different carbonisation temperatures

Sample	Adsorption capacity (mg/g)
EFBC-400	0.584
EFBC-450	0.340
EFBC-500	0.323
EFBC-550	0.137

Apparently, such characteristics are better for NO removal by EFBC, similar to Claudino *et al.* who reported a higher NO adsorption by PK35 with smaller average micropore width (about 2.24 nm) apart from the role of oxygen functionality groups in NO removal [33]. On the other hand, Kaneko *et al.* reported that the optimum pore diameter for NO adsorption is 0.6–1.1 nm based on micropore filling of supercritical NO [34], which is even smaller than the pore diameter of EFBC-400 in this work (2.78 nm).

In addition, a previous work explained that an appropriate size of micropores is required for NO removal from a kinetic point of view [35]. The size and the shape of the pores can greatly influence the accessibility to the carbon's internal area, thereby improving the mass transport of reacting gas from the exterior surface to an active site beneath the surface and transport of products in the opposite direction [36]. The significance of microporous structure for NO removal is also supported by several previous studies

including a study on waste-derived activated carbons for control of nitrogen oxides [37].

4.0 CONCLUSION

Chemical activation of oil palm empty fruit bunch (EFB) biomass using H_3PO_4 produced porous activated carbon with BET surface area ranging from 215 to 759 m^2/g . All EFBC samples showed an increase in the surface area and total pore volume with an increase in carbonisation temperature from 400 to 550°C. EFBC carbonised at a lower temperature (400°C) was found to exhibit a microporous structure with 98% of micropores, favouring NO removal at low temperature (100°C) than the rests (carbonised at 450-550°C). As the carbonisation temperature rises, the pores were enlarged, becoming more mesoporous and less uniform while the heterogeneity of pores was increased. This slightly decreased the NO adsorption capacity from 0.58 to 0.14 mg/g. It can thus be suggested that a proper pore size of EFBC is important in the kinetics of NO adsorption, by improving the accessibility of NO to the internal area of the carbon. Future work will include an evaluation of the kinetics of NO removal through application of various kinetic models including Avrami's and intra-particle diffusion, as well as a study on EFBC regeneration.

Acknowledgement

The authors acknowledge the financial support provided by Ministry of Education Malaysia from the Fundamental Research Grant Scheme (FRGS) under a grant number of FRGS/2/2013/SG01/UNIMAP/02/1.

References

- [1] Wang, C., P. Guo, G. Han, X. Feng, P. Zhang, and X. Tian. 2010. Effect of Simulated Acid Rain on the Litter Decomposition of *Quercus Acufissima* and *Pinus Massoniana* in Forest Soil Microcosms and the Relationship with Soil Enzyme Activities. *Science of the Total Environment*. 408(13): 2706-2713. DOI: 10.1016/j.scitotenv.2010.03.023.
- [2] Walid Bizreh, Y., L. Al-Hamoud, and M. AL-Joubeh. 2014. A Study on the Catalytic Activity of New Catalysts for Removal of NO_x, CH and CO Emitted from Car Exhaust. *Journal of the Association of Arab Universities for Basic and Applied Sciences*. 16: 55-63. DOI: 10.1016/j.jaubas.2013.06.001.
- [3] Sych, N. V., S. I. Trofymenko, O. I. Poddubnaya, M. M. Tsyba, V. I. Sapsay, D. O. Klymchuk, and A. M. Puziy. 2012. Porous Structure and Surface Chemistry of Phosphoric Acid Activated Carbon from Corn cob. *Applied Surface Science*. 261: 75-82. DOI: 10.1016/j.apsusc.2012.07.084.
- [4] Guo, S., J. Peng, W. Li, K. Yang, L. Zhang, S. Zhang, and H. Xia. 2009. Effects of CO₂ Activation on Porous Structures of Coconut Shell-based Activated Carbons. *Applied Surface Science*. 255(20): 8443-8449. DOI: 10.1016/j.apsusc.2009.05.150.
- [5] Rashidi, N. A., S. Yusup, and L. H. Loong. 2013. Kinetic Studies on Carbon Dioxide Capture using Activated Carbon. *Chemical Engineering Transactions*. 35: 361-366. DOI: 10.3303/CET1335060.
- [6] Guo, J., and A. C. Lua. 2003. Textural and Chemical Properties of Adsorbent Prepared from Palm Shell by Phosphoric Acid Activation. *Materials Chemistry and Physics*. 80: 114-119. DOI: 10.1016/S0254-0584(02)00383-8.
- [7] Do, D. D., and A. Ahmadpour. 1995. The Preparation of Active Carbons from Coal by Chemical and Physical Activation. *Carbon*. 34(4): 471-479. DOI:10.1016/0008-6223(95)00204-9.
- [8] Li, W., K. Yang, J. Peng, L. Zhang, S. Guo, and H. Xia. 2008. Effects of Carbonization Temperatures on Characteristics of Porosity in Coconut Shell Chars and Activated Carbons Derived from Carbonized Coconut Shell Chars. *Industrial Crops and Products*. 28(2): 190-198. DOI: 10.1016/j.indcrop.2008.02.012.
- [9] Gratuito, M. K. B., T. Panyathanmaporn, R. A. Chumnanklang, N. Sirinuntawittaya, and A. Dutta. 2008. Production of Activated Carbon from Coconut Shell: Optimization using Response Surface Methodology. *Bioresour Technol*. 99(11): 4887-4895. DOI: 10.1016/j.biortech.2007.09.042.
- [10] Mane, V. S. and P. V. V Babu. 2011. Studies on the Adsorption of Brilliant Green Dye from Aqueous Solution onto Low-cost NaOH Treated Saw Dust. *Desalination*. 273(2-3): 321-329. DOI: 10.1016/j.desal.2011.01.049.
- [11] Lau, L. C., K. T. Lee, and A. R. Mohamed. 2010. Rice Husk Ash Sorbent Doped with Copper for Simultaneous Removal of SO₂ and NO: Optimization Study. *Journal of Hazardous Materials*. 183(1-3): 738-45. DOI: 10.1016/j.jhazmat.2010.07.088.
- [12] Njoku, V. O., K. Y. Foo, M. Asif, and B. H. Hameed. 2014. Preparation of Activated Carbons from Rambutan (*Nephelium lappaceum*) Peel by Microwave-induced KOH Activation for Acid Yellow 17 Dye Adsorption. *Chemical Engineering Journal*. 250: 198-204. DOI:10.1016/j.cej.2014.03.115.
- [13] Prauchner, M. J., and F. Rodríguez-Reinoso. 2012. Chemical Versus Physical Activation of Coconut Shell: A Comparative Study. *Microporous and Mesoporous Materials*. 152(2012): 163-171. DOI:10.1016/j.micromeso.2011.11.040.
- [14] Qin, C., Y. Chen, and J. Gao. 2014. Manufacture and Characterization of Activated Carbon from Marigold Straw (*Tagetes Erecta* L.) by H_3PO_4 Chemical Activation. *Materials Letters*. 135: 123-126. DOI: 10.1016/j.matlet.2014.07.151.
- [15] Wang, X., D. Li, W. Li, J. Peng, H. Xia, L. Zhang, S. Guo, and G. Chen. 2013. Optimization of Mesoporous Activated Carbon from Coconut Shells by Chemical Activation with Phosphoric Acid. *Bioresour Technol*. 8(4): 6184-6195. DOI: 10.15376/biores.8.4.6184-6195.
- [16] Xue, Y., Y. Guo, Z. Zhang, Y. Guo, Y. Wang, and G. Lu. 2008. The Role of Surface Properties of Activated Carbon in the Catalytic Reduction of NO by Carbon. *Applied Surface Science*. 255(5): 2591-2595. DOI: 10.1016/j.apsusc.2008.07.167.
- [17] Xue, Y., G. Lu, Y. Guo, Y. Guo, Y. Wang, and Z. Zhang. 2008. Effect of Pretreatment Method of Activated Carbon on the Catalytic Reduction of NO by Carbon over CuO. *Applied Catalysis B: Environmental*. 79(3): 262-269. DOI: 10.1016/j.apcatb.2007.10.027.
- [18] Yin, C., M. Aroua, and W. Daud. 2007. Review of Modifications of Activated Carbon for Enhancing Contaminant Uptakes from Aqueous Solutions. *Separation and Purification Technology*. 52(3): 403-415. DOI: 10.1016/j.seppur.2006.06.009.
- [19] Rafatullah, M., O. Sulaiman, R. Hashim, and A. Ahmad. 2010. Adsorption of Methylene Blue on Low-cost

- Adsorbents: A Review. *Journal of Hazardous Materials*. 177(1-3): 70-80.
DOI: 10.1016/j.jhazmat.2009.12.047.
- [20] Ghouma, I., M. Jeguirim, L. Limousy, N. Bader, A. Ouederni, and S. Bennici. 2018. Factors influencing NO₂ Adsorption/reduction on Microporous Activated Carbon: Porosity vs. Surface Chemistry. *Materials*. 11(4): 622-640.
DOI: 10.3390/ma11040622.
- [21] Belhachemi, M., M. Jeguirim, L. Limousy, and F. Addoun. 2014. Comparison of NO₂ Removal Using Date Pits Activated Carbon and Modified Commercialized Activated Carbon via Different Preparation Methods: Effect of Porosity and Surface Chemistry. *Chemical Engineering Journal*. 253(2): 121-129.
DOI: 10.1016/j.cej.2014.05.004.
- [22] Nowicki, P., R. Pietrzak, and H. Wachowska. 2010. Sorption Properties of Active Carbons Obtained from Walnut Shells by Chemical and Physical Activation. *Catalysis Today*. 150(1-2): 107-114.
DOI: 10.1016/j.cattod.2009.11.009.
- [23] Cha, J. S., J. C. Choi, J. H. Ko, Y. K. Park, S. H. Park, K. E. Jeong, S. S. Kim, and J. K. Jeon. 2010. The Low-temperature SCR of NO over Rice Straw and Sewage Sludge Derived Char. *Chemical Engineering Journal*. 156(2): 321-327.
DOI: 10.1016/j.cej.2009.10.027.
- [24] Rosas, J. M., J. Bedia, J. Rodriguez-Mirasol, and T. Cordero. 2010. On the Preparation and Characterization of Chars and Activated Carbons from Orange Skin. *Fuel Processing Technology*. 91(10): 1345-1354.
DOI: 10.1016/j.fuproc.2010.05.006.
- [25] Sumathi, S., S. Bhatia, K. T. Lee, and A. R. Mohamed. 2009. Performance of an Activated Carbon Made from Waste Palm Shell in Simultaneous Adsorption of SO_x and NO_x of Flue Gas at Low Temperature. *Science in China Series E: Technological Sciences*. 52(1): 198-203
DOI: 10.1007/s11431-009-0031-6.
- [26] Pietrzak, R., P. Nowicki, J. Kązmierczak, I. Kuszyńska, J. Goscińska, and J. Przepiórski. 2014. Comparison of the Effects of Different Chemical Activation Methods on Properties of Carbonaceous Adsorbents obtained from Cherry Stones. *Chemical Engineering Research and Design*. 92(6): 1187-1191.
DOI: 10.1016/j.cherd.2013.10.005.
- [27] Ng, W. P. Q., H. L. Lam, F. Y. Ng, M. Kamal, and J. H. E. Lim. 2012. Waste-to-wealth: Green Potential from Palm Biomass in Malaysia. *Journal of Cleaner Production*. 34: 57-65.
DOI: 10.1016/j.jclepro.2012.04.004.
- [28] Ahmad, N., S. H. Yong, N. Ibrahim, U. F. M. Ali, F. M. Ridwan, and R. Ahmad. 2018. Optimisation of Copper Oxide Impregnation on Carbonised Oil Palm Empty Fruit Bunch for Nitric Oxide Removal using Response Surface Methodology. *E3S Web of Conferences*. 02029.
DOI: 10.1051/e3sconf/20183402029.
- [29] Guo, Y., and D. A. Rockstraw. 2007. Activated Carbons Prepared from Rice Hull by One-step Phosphoric Acid Activation. *Microporous and Mesoporous Materials*. 100(1-3): 12-19.
DOI: 10.1016/j.micromeso.2006.10.006.
- [30] Ahmad, M. A., W. M. A. Wan Daud, and M. K. Aroua. 2008. Adsorption Kinetics of Various Gases in Carbon Molecular Sieves (CMS) Produced from Palm Shell. *Colloids and Surfaces A: Physicochemical and Engineering Aspects*. 312(2-3): 131-135.
DOI: 10.1016/j.colsurfa.2007.06.040.
- [31] Sudaryanto, Y., S. B. Hartono, W. Irawaty, H. Hindarso, and S. Ismadi. 2006. High Surface Area Activated Carbon Prepared from Cassava Peel by Chemical Activation. *Bioresource Technology*. 97(5): 734-739.
DOI: 10.1016/j.biortech.2005.04.029.
- [32] Bazan-Wozniak, A., P. Nowicki, and R. Pietrzak. 2017. The Influence of Activation Procedure on the Physicochemical and Sorption Properties of Activated Carbons Prepared from Pistachio Nutshells for Removal of NO₂/H₂S gases and dyes. *Journal of Cleaner Production*. 152: 211-222.
DOI: 10.1016/j.jclepro.2017.03.114.
- [33] Claudino, A., J. L. Soares, R. F. P. M. Moreira, and H. J. José. 2004. Adsorption Equilibrium and Breakthrough Analysis for NO Adsorption on Activated Carbons at Low Temperatures. *Carbon*. 42(8-9): 1483-1490.
DOI: 10.1016/j.carbon.2004.01.048.
- [34] Kaneko, K., N. Fukuzaki, K. Kakei, T. Suzuki, and Sumio Ozeki. 1989. Enhancement of NO Dimerization by Micropore Fields of Activated Carbon Fibers. *Langmuir*. 5: 960-965.
DOI: 10.1021/la00088a014.
- [35] Alcañiz-Monge, J., A. Bueno-López, M.Á. Lillo-Rodenas, and M. J. Illán-Gómez. 2008. No Adsorption on Activated Carbon Fibers from Iron-containing Pitch. *Microporous and Mesoporous Materials*. 108(1-3): 294-302.
DOI: 10.1016/j.micromeso.2007.04.011.
- [36] Linares-solano, A. 1989. Textural Characterization of Porous Carbons. *Carbon and Coal Gasification*. Martinus Nijhoff Publishers, Dordrecht. 137-178.
- [37] Al-Rahbi, A. S. S., M. A. Nahil, C. Wu, and P. T. Williams. 2016. Waste-derived Activated Carbons for Control of Nitrogen Oxides. *Proceedings of the Institution of Civil Engineers-Waste and Resource Management*. 169(1): 30-41.
DOI: 10.1680/jwarm.14.00021.